Desalination and Water Treatment
www.deswater.com

doi: 10.5004/dwt.2021.27327

228 (2021) 444–455
July

Prediction of groundwater depth based on CEEMD-BP coupling model in irrigation area

Xianqi Zhang[a,b,c], Tao Wang[a,*], Shaoyu He[a]

[a]*Water Conservancy College, North China University of Water Resources and Electric Power, Zhengzhou 450046, China, emails: 1124149584@qq.com (T. Wang), zxqi@163.com (X. Zhang), 840515956@qq.com (S. He)*
[b]*Collaborative Innovation Center of Water Resources Efficient Utilization and Protection Engineering, Zhengzhou 450046, China*
[c]*Technology Research Center of Water Conservancy and Marine Traffic Engineering, Henan Province, Zhengzhou 450046, China*

Received 25 December 2020; Accepted 12 April 2021

ABSTRACT

Accurate prediction of groundwater depth has guiding value for the rational use of water and soil resources in irrigation areas. The buried depth of groundwater is a complex system, and its evolution is characterized by nonlinearity and non-stationarity. Complementary ensemble empirical mode decomposition (CEEMD) is one of the methods of "decomposition–prediction–reconstruction" predictive model, and its data decomposition has a certain inhibitory effect on the modal alias problem in the process of empirical mode decomposition. Based on CEEMD, it has the ability to smooth non-stationary signals and back-propagation (BP) can approximate arbitrary functions, has good nonlinear mapping capabilities, and has an advantage in the prediction of uncertain factors. This paper builds a coupling model based on the groundwater depth prediction of CEEMD-BP and applies it to the groundwater depth prediction of People's Victory Canal Irrigation District. The results show that the CEEMD-BP coupling model has a good predictive effect, with an average relative error of 4.7% and an inter-rate agreement of 100%. Which is superior to the EEMD-BP model and the BP model, and it has a higher fitting and predicted accuracy. Providing an effective prediction method of application prospects for the buried depth of groundwater in the irrigation area.

Keywords: BP network; Complementary ensemble empirical mode decomposition; Groundwater depth; People's Victory Canal Irrigation District; Prediction

1. Introduction

Groundwater burial depth variation in irrigation areas is a complex, fuzzy and uncertain system, influenced by various factors such as temperature, precipitation, evapotranspiration dispersion [1], groundwater recharge, groundwater extraction, soil geological conditions, etc., resulting in groundwater burial depth variation showing non-linearity, non-smoothness, local volatility and multi-temporal [2–4]. It makes the prediction of groundwater depth of burial more difficult and requires more demanding prediction methods. For this reason, the introduction of artificial neural networks with better non-linear and self-learning capabilities for groundwater burial depth prediction has become a new topic of research for scholars at home and abroad. Adhikary and Dash [5] used cross-validation methods to compare the effectiveness of Inverse Distance Weighting (IDW), Radial Basis Function (RBF), Ordinary Kriging (OK), and Universal Kriging (UK) interpolation methods in groundwater level prediction. Al-Mahallawi et al. [6] used neural networks to predict changes in nitrate pollution of groundwater in rural

* Corresponding author.

agricultural areas. Sucharita et al. [7] used the use of different heuristic models to evaluate the prediction of groundwater burial depth across basins in India. Khorasani et al. [8] used time series models for groundwater depth of burial prediction. Maiti et al. [9] used artificial neural networks and neuro-fuzzy models for groundwater level prediction. Liu et al. [10] used artificial neural networks in complex groundwater management. Zhou et al. [11] combined wavelet pre-processing of artificial neural network and support vector machine models for comparative analysis of groundwater depth prediction. Shao et al. [12] used an Improved Artificial Bee Colony (IABC)-RBF neural network to predict groundwater depth, which improved the learning speed of the network and improved the prediction capability of the neural network. Zhang et al. [13] used a long and short term memory network to simulate the variation of groundwater depth in Guanzhong well. Yu et al. [14] used a coupled wavelet transform and support vector machine model (WA-SVM) to predict the burial depth of groundwater in arid areas, which can provide new methods and ideas for dynamic prediction of groundwater burial depth in arid areas. Liang et al. [15] constructed an EEMD-PSO-ELM (PSO – Particle Swarm Optimization; ELM – Extreme Learning Machine) groundwater depth prediction model to predict the monthly groundwater depth of Youyi Farm, which can provide a basis for groundwater management and agricultural policy formulation in Youyi Farm and even in the Sanjiang Plain. As can be seen from the above, researchers at home and abroad have mainly studied groundwater burial depth prediction models through artificial neural networks or machine learning methods. The construction of coupled prediction models by reducing the non-smoothness of the original series is less common. Complementary ensemble empirical mode decomposition (CEEMD) [16] transforms complex time series variations into a few simple. The method is used to smooth non-smoothed series by extracting the Intrinsic Model Function (IMF) from the original signal, thereby separating the low and high frequency parts of the signal and transforming the complex time series variation into the sum of a few simple variables. In this paper, CEEMD is used to decompose the groundwater burial depth data, and the decomposed series has good smoothness. Combined with back propagation (BP) neural network which can approximate arbitrary functions and has good nonlinear mapping ability, it has advantages in prediction of uncertainty factors [17]. A coupled CEEMD-BP neural network model for groundwater burial depth prediction in the People's Victory irrigation area was established to reveal the predictive capability of the coupled model for groundwater burial depth in the irrigation area. A new approach is provided for the improvement of groundwater burial depth prediction accuracy. In addition, the analysis-prediction of the periodic characteristics of groundwater burial depth can provide data support for the rational use of groundwater resources, which has important guidance significance for social and economic development.

In order to improve the accuracy of groundwater depth prediction, this paper proposes to combine the CEEMD method of the BP neural network to predict the groundwater depth. By combining with the EEMD-BP model, the BP model and the Elman model, the relative percentage error (RPE) and the average absolute percentage error (MAPE), root mean square error (RMSE), average absolute error (MAE) and Nash coefficient (NSE) and other indicators are compared to analyze the effectiveness of the CEEMD-BP model for groundwater depth prediction.

2. Basic principles and methods

2.1. Complementary ensemble empirical mode decomposition

Empirical mode decomposition (EMD) [18] is a signal decomposition based on the time-scale characteristics of the data itself, which has obvious advantages for handling non-stationary and non-linear data. EEMD is an improved algorithm of empirical mode decomposition. Compared with EMD, EEMD adds Gaussian white noise to the signal to change the characteristics of the extremum point, so that the signal has continuity at different scales and effectively suppresses the phenomenon of confounding in EMD decomposition, but the addition of white noise will remain in the component signal and cause signal reconstruction errors.

Different from the EEMD method, CEEMD adds white noise with an opposite mean value of 0 to the original signal, so that CEEMD have features not only reduces the non-stationarity of the sequence, but also transforms the non-stationary time series into a stable and minimally influential sequence [19]. Moreover, the addition of white noise that is opposite to each other reduces signal errors of reconstruction, minimizes the interference from white noise on the signal decomposition, and have a better completeness of the decomposition.

The implementation steps of CEEMD decomposition are as follows:

1. In the original time series, randomly add n sets of positive and negative auxiliary white noise sequences with a mean value of zero to generate two sets of aggregate signals.

$$\begin{bmatrix} G_1 \\ G_2 \end{bmatrix} = \begin{bmatrix} 1 & 1 \\ 1 & -1 \end{bmatrix} \begin{bmatrix} S \\ N \end{bmatrix} \tag{1}$$

   where G_1 and G_2 are the time-series signals after adding positive and negative white noise; N is the auxiliary noise signal and S is the original signal. Finally, there are $2n$ sets of signals were obtained [20].
2. The EMD decomposition method is used to decompose each set signal, and each signal gets a set of $2m-1$ IMF components and a trend term, where the jth IMF component of the ith component represents c_{ij}. m is the number of signals after each signal is decomposed.
3. Take the average of the corresponding IMF components and trend items as the final decomposition.

$$U(t) = \sum_{j=1}^{l} c_j + \sum_{j=l+1}^{m} c_j + r_m \tag{2}$$

   where $U(t)$ represents the sum of IMF components and the remaining components after CEEMD decomposition of the original noisy data, and r_m represents the average trend or constant.

2.2. BP neural network

BP neural network usually adopts the structure of multi-layer forward neural network based on BP neuron, which is composed of input layer, hidden layer and output layer, and each layer has several neurons. The BP network divides the entire learning process into two parts, namely the forward propagation of the network input signal and the backward propagation of the error signal. The network is trained in the learning method with a tutor. In the forward propagation, the input signal is passed from the input layer to the output layer through the hidden layer calculated layer by layer; in the output layer, the output of each neuron corresponds to the network response of the input mode. If the output layer does not get the expected output, the error turn to back propagation, following the principle of reducing the inaccuracy between the expected output and the actual output, the error information of each unit is returned from the output layer to the input layer through the middle layer. The connection weights and thresholds are modified layer by layer, and the cycle is repeated until the error signal reaches the allowable range or the number of exercises reaches the predetermined number [21–23]. A schematic diagram of the network is shown in Fig. 1.

The action function of the node usually selects the Sigmoid type function, and its expression is:

$$f(x)=\frac{1}{1+e^{-x}} \tag{3}$$

where $f(x)$ is the function of the network node; x is the input value of the neuron node.

The programming steps of the standard BP algorithm are:

1. Perform data normalization. All sample data are normalized by the normalisation functions.
2. Initialization. Assign random numbers to the weight matrix W and V, set the sample pattern counter P and the training times counter q to 1, the error E to 0, the learning rate η to a decimal within 0–1, and the accuracy $E_{\min}$ to be achieved after network training a positive decimal.
3. Input the training sample pair and calculate the output of each layer. Use the current samples X^P and d^P to assign values to the vector arrays X and d, and use the following formula to calculate the components in the hidden layer Y and the output layer O.

$$O_k = f\left(\text{net}_k\right) \quad k=1,2,\ldots,l \tag{4}$$

$$\text{net}_k = \sum_{j=0}^{m}\omega_{jk}y_j \quad k=1,2,\ldots,l \tag{5}$$

$$y_j = f\left(\text{net}_j\right) \quad j=1,2,\ldots,m \tag{6}$$

$$\text{net}_j = \sum_{i=0}^{n}v_{ij}x_i \quad j=1,2,\ldots,m \tag{7}$$

4. Calculate the network output error. Suppose there is p pairs of training samples, and the network has different errors E^P for different samples. The squares of the output errors of all samples can be accumulated and then squared as the total output error. $E_{\max}$, the largest of the errors, can also be used to represent the total network output error, the root mean square error is often used as the total error of the network in practical applications.
5. Calculate the error signal of each layer. Apply formula (4) to calculate δ_k^0 and δ_j^y.

$$\delta_k^0 = \left(d_k - o_k\right)o_k\left(1-o_k\right) \tag{8}$$

$$\delta_j^y = \left(\sum_{k=1}^{l}\delta_k^0\omega_{jk}\right)y_j\left(1-y_j\right) \tag{9}$$

6. Adjust the weights of each layer. Use the following formula to calculate each component of W and V.

$$\Delta\omega_{jk} = \eta\delta_k^0 y_j = \eta\left(d_k - o_k\right)o_k\left(1-o_k\right)y_j \tag{10}$$

$$\Delta v_{ij} = \eta\delta_j^y x_i = \eta\left(\sum_{k=1}^{l}\delta_k^0\omega_{jk}\right)y_j\left(1-y_j\right)x_i \tag{11}$$

7. Check whether one rotation training is completed for all samples. If $p < P$, the counters p and q increases by 1, and return to step (3), otherwise, go to step (8).

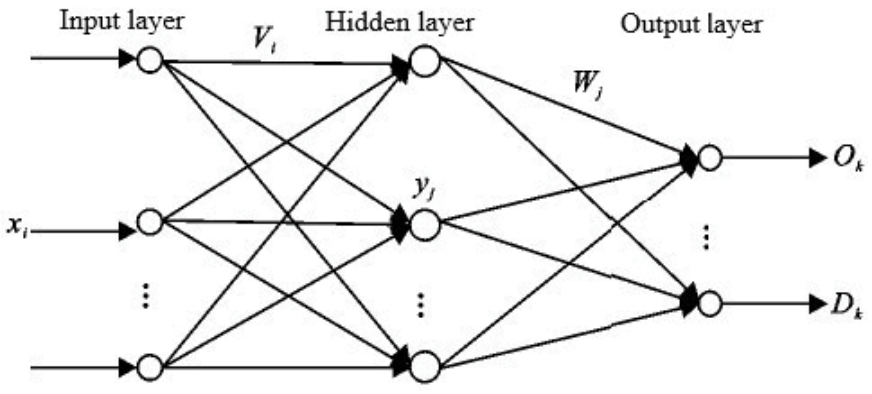

Fig. 1. The BP neural network structure.

8. Check whether the total error of the network meet the accuracy requirements. When using ERME as the total error of the network, if $E_{RME} < E_{min}$, the training ends, otherwise E is set to 0, p is set to 1, and step (3) is returned.

3. Coupling model

3.1. CEEMD-BP

From the perspective of CEEMD decomposition, the contribution rate of each IMF component and trend relative to the time series is not the same. The IMF component and trend term can be approximately regarded as the driving factors of time. So that the time forecast is equivalent to the forecast of IMF components and trend items.

The specific steps of CEEMD-BP coupling model are as follows:

1. CEEMD decomposition. Use MATLAB to decompose the original data by CEEMD to get the IMF components and trend items of the time series.
2. Divide training data and prediction data. The IMF components and trend items of the groundwater depth from 1993 to 2011 are used as the training data of the BP network, and the IMF components and trend items from 2012 to 2013 are used as the prediction data of the BP network.
3. BP neural network prediction. The BP network is used to repeatedly debug the training data of IMF components and trend items, so that the prediction of BP components and trend items reaches the best effect.
4. Analysis of prediction results. Finally, the predicted IMF components and trend items are cumulatively restored and compared with the original data.

The technical route of CEEMD-BP coupling prediction model is shown in Fig. 2.

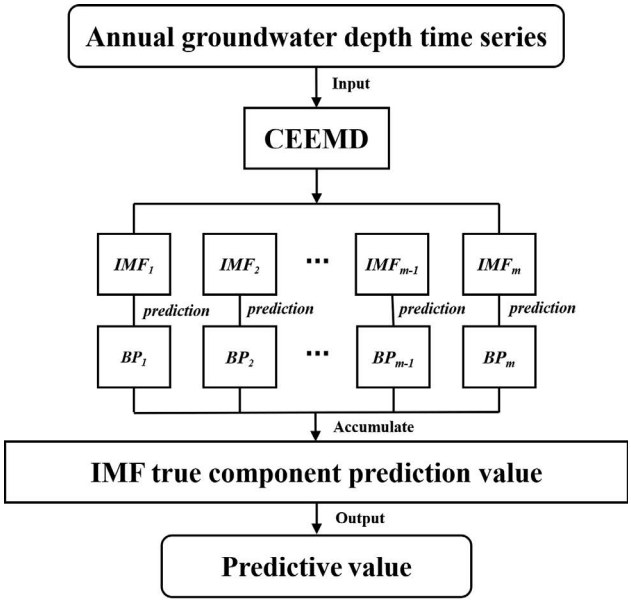

Fig. 2. The technical route of the CEEMD-BP coupling prediction model.

3.2. Evaluation index

In order to better reflect the prediction effect of the CEEMD-BP model, five main criteria are used for evaluation of prediction, relative percentage error (RPE), average absolute error (MAE), root mean square error (RMSE), average relative percentage error (MAPE), and Nash efficiency coefficient (NSE), which are defined as:

$$\mathrm{RPE} = \frac{\left|y_t - \bar{y}_t\right|}{y_t} \times 100\% \tag{12}$$

$$\mathrm{MAE} = \frac{1}{N}\sum_{t=1}^{N}\left|y_t - \bar{y}_t\right| \tag{13}$$

$$\mathrm{RMSE} = \sqrt{\frac{1}{N}\sum_{t=1}^{N}\left(y_t - \bar{y}_t\right)^2} \tag{14}$$

$$\mathrm{MAPE} = \frac{1}{N}\sum_{t=1}^{N}\left|\frac{y_t - \bar{y}_t}{y_t}\right| \times 100\% \tag{15}$$

$$\mathrm{NSE} = 1 - \frac{\sum_{t=1}^{N}\left(y_t - \bar{y}_t\right)^2}{\sum_{t=1}^{N}\left(y_t - \mu_t\right)^2} \tag{16}$$

where y_t is the actual value of the t moment; $\bar{y}_t$ is the prediction value of the t moment; μ_t is the total average value of observations at time t; N is the number of time series.

4. Example application

4.1. Regional overview

The People's Victory Canal Irrigation District is located in the northern part of Henan Province. It is the first large-scale artesian irrigation district built on the lower Yellow River since the founding of New China. In recent years, with the completion and use of Xiaolangdi Reservoir, the intake of the People's Victory Canal Irrigation District has difficulty diverting water due to the elevation of the sluice bottom. The development of industry and agriculture and the improvement of urbanization in the irrigation area have an increasing demand for water resources, so groundwater exploitation has been gradually increased, becoming one of the main water sources in the irrigation area.

The irrigation area has a warm temperate continental monsoon climate, with an average annual temperature of 140°C, a frost-free period of 220 d, an average annual water surface evaporation of 1,300 mm, and an annual average precipitation of 620 mm. The total land area in the irrigation area is 1,486.84 km^2. The data in this article comes from the monthly monitoring data of observation wells in the irrigation area from 1993 to 2013.

It can be seen from Fig. 3 that from 1993 to 2013, the groundwater depth of the People's Victory Canal Irrigation District showed an upward trend. The rising process was accompanied by certain fluctuations and the fluctuation

range was inconsistent. This also verified the uncertainty and non-stationarity of the groundwater depth sequence is relatively large, which T also reflects the rationality of choosing the CEEMD method from the side.

4.2. CEEMD decomposition

According to the previous CEEMD decomposition steps, the groundwater depth data of the People's Victory Canal Irrigation District from 1993 to 2013 was subjected to CEEMD decomposition, with the noise variance being 0.2 and the number of noise being 100. The decomposition result is shown in Fig. 4.

It can be seen from Fig. 4 that the groundwater depth sequence is decomposed into 5 IMF components and a corresponding trend item. Among them, the IMF1 component has the largest volatility, high frequency, and the shortest wavelength; the amplitude of IMF2 ~ trend phase gradually decreases, the frequency gradually decreases, and the wavelength gradually increases. After the groundwater depth sequence of the People's Victory Canal Irrigation District is processed by CEEMD, the volatility and non-stationarity of the sequence are greatly reduced, and the original

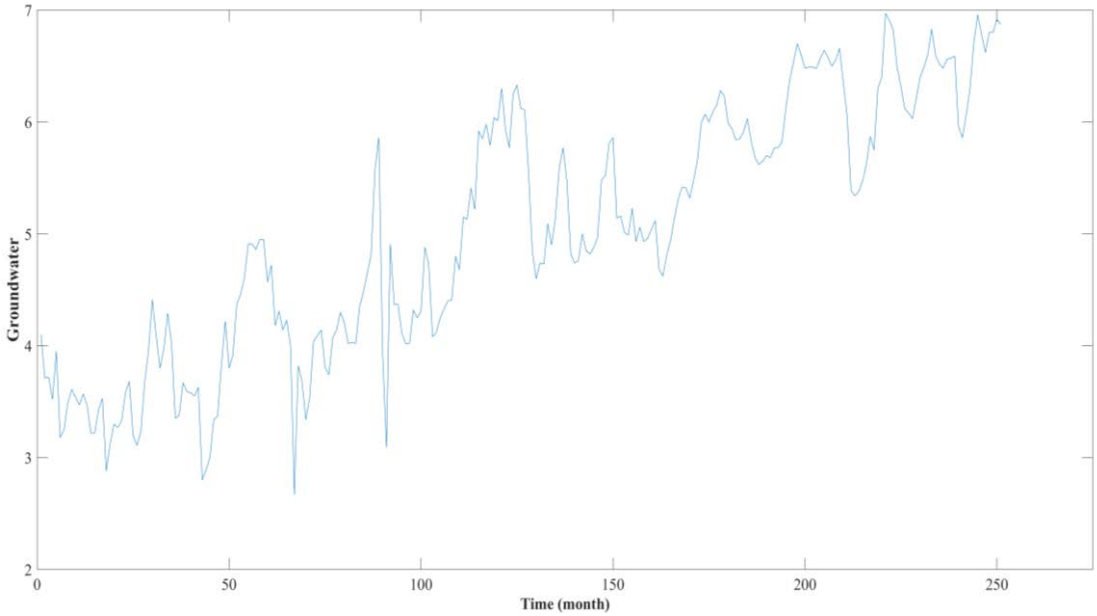

Fig. 3. Groundwater depth curve of the people's victory canal irrigation district from 1993 ~ 2013.

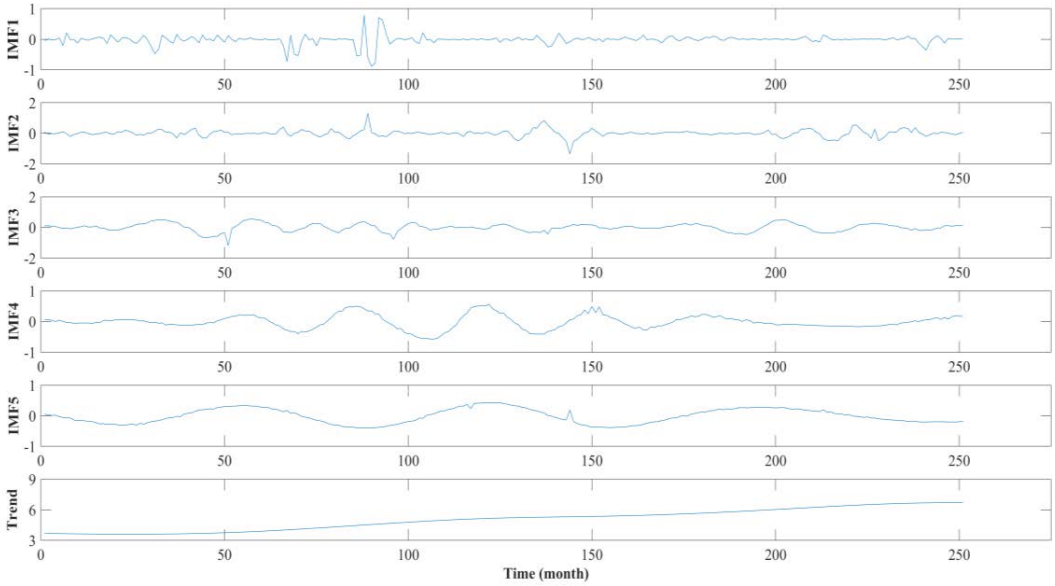

Fig. 4. CEEMD decomposition of groundwater depth in the People's Victory Canal Irrigation District from 1993 ~ 2013.

sequence is decomposed into periodic IMF components to reduce the difficulty of prediction.

4.3. Groundwater depth prediction

When using BP network to predict the depth of groundwater in People's Victory Canal Irrigation District, training and testing samples must be divided. The IMF and trend items from 1993 to 2011 are used as training samples, and the IMF and trend items from 2012 to 2013 are used as test samples. Using the rolling prediction method, the delay order is 1:6, and the number of hidden nodes is 20.

According to the previous steps, the BP network is used to predict the five IMF components and one trend item of the groundwater depth in the People's Victory Canal Irrigation District from 2012 to 2013. The prediction results are shown in Figs. 5a–f.

It can be seen from Figs. 5a–f that the prediction effect of the IMF1 component is slightly worse, which indicates that the non-stationarity of the IMF1 component is higher; the prediction effect of IMF2 ~ IMF6 is better, which shows that the non-stationarity of the IMF2 ~ IMF6 components is lower, after the groundwater depth sequence is decomposed by CEEMD, the volatility and non-stationarity of the sequence are greatly reduced.

It can be seen from Table 1 that the maximum, minimum, and average values of IMF1 relative errors are relatively large, which are 594.74, 4.30, and 161.55, respectively, which shows that the non-stationarity of the IMF1 component is higher and has a greater impact on the prediction error; The maximum, minimum, and average values of the relative error are small, respectively 0.04, 0.00, 0.01, which shows that the low-frequency signal is relatively stable and has little effect on the prediction error. It can be seen from Table 1 that after the groundwater depth sequence is decomposed by CEEMD, the IMF component becomes more and more stable, and the indicators of the relative error of the IMF1 residual show a decreasing trend overall.

It can be seen from Table 2 that the maximum, minimum, and average relative errors of the CEEMD-BP coupling prediction model is 3.04%, 0.03%, and 0.73%, respectively, and the Nash efficiency coefficient of the model is calculated to be 0.96, which is close to 1 which shows that the quality of the model is very high, the relative error of model prediction are small, and the qualification rate is high.

Fig. 6 is the prediction curve of groundwater depth in People's Victory Canal Irrigation District from 2012 to 2013. It can be seen from Fig. 7 that the predicted value of groundwater depth in People's Victory Canal Irrigation District from 2012 to 2013 is basically the same as the real value. The degree of fitting of CEEMD-BP coupling model is higher.

5. Results and discussion

In order to further evaluate the function of the proposed model, the simulation results of several models in the prediction of groundwater depth are compared. Due to the limited mastery of various forecasting methods, only the simulation results of Elman, EEMD-BP, BP and CEEMD-BP are compared as shown below.

Fig. 7 compares the reconstruction error of CEEMD and EEMD. It can be clearly seen that the reconstruction error of EEMD is much larger than that of CEEMD; the CEEMD-BP coupling model better overcomes the shortcomings of white noise for the large reconstruction error of the EEMD-BP network.

It can be seen from Table 3 and Fig. 8 that the CEEMD-BP coupling model has the highest degree of fitting for groundwater depth prediction, and MAE, RMSE, and MAPE are all lower than the other three prediction models; the BP prediction model has a higher degree of fitting Based on the Elman prediction model; at the same time, it can be seen that the prediction effect of the "decomposition–prediction–reconstruction" model is significantly better than that of a single neural network prediction model; the original signal is decomposed to reduce the non-stationarity of the sequence, thereby improving the prediction accuracy.

It can be seen from Fig. 9 that when predicting a total of 24 months from 2012 to 2013, 73% of the relative error of CEEMD-BP is less than that of the other three models, and CEEMD-BP model possesses more effective prediction.

From the above comparative analysis, it can be concluded that the CEEMD-BP model prediction results are as expected, and the period and trend are in high agreement with the sequence of the measured data. The relative error sum is lower and the results are better compared to Elman, EEMD-BP and BP, which indicates that CEEMD-BP is more advantageous for precipitation forecasting. Compared to other forecasting methods, decomposing the reconstructed forecast model reduces the forecast error. The reason for this is as follows: the original signal is decomposed by a decomposition tool (CEEMD) into different frequency components of the high-frequency and low-frequency components. The overall prediction error of the model is determined by the error predictions of these high-frequency and low-frequency components. In this way, even if some components are not predicted well, the overall prediction is not affected.

CEEMD is proposed on the basis of EEMD. The CEEMD decomposition solves the problems of modal confusion and residual noise in the reconstructed sequence that exist in the EEMD decomposition process, and its decomposition process has integrity and no reconstruction error. Therefore, the prediction effect of CEEMD-BP model is more advantageous and stable than the single decomposition reconstruction prediction model of EEMD-BP.

6. Conclusion

1. The groundwater depth sequence is decomposed by CEEMD, by adding opposite white noises whose average value are equal to 0, solves the problem of large reconstruction errors caused by adding single row white noise to EEMD decomposition. The time series of groundwater depth is decomposed by CEEMD, the signal is decomposed into 5 IMF components and trend items, the predicted value of the signal is equal to the sum of the predicted values of the 5 IMF components and the trend item. By decomposing the groundwater depth sequence into different frequency subcomponents, the complex groundwater depth prediction becomes a prediction of many simple single variables. Reducing the

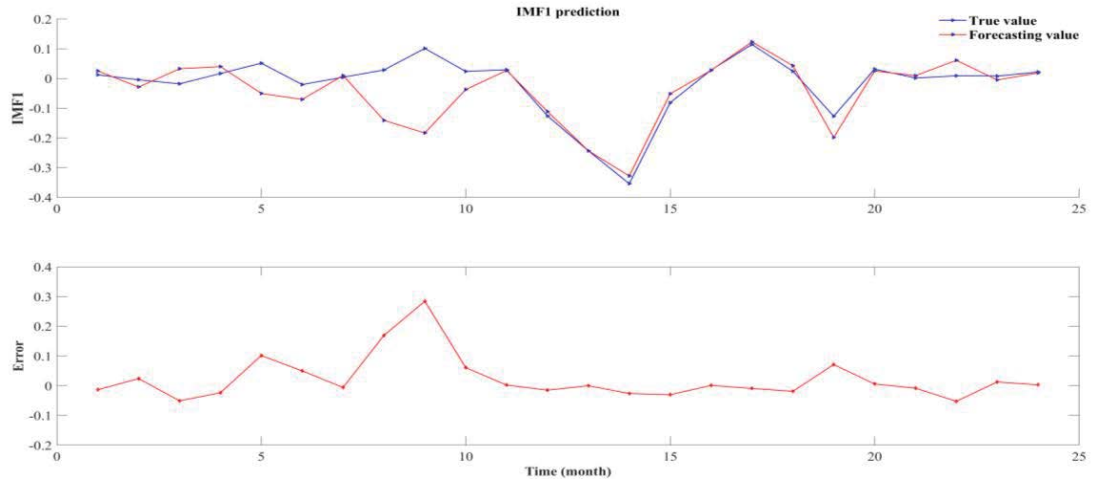

(a)

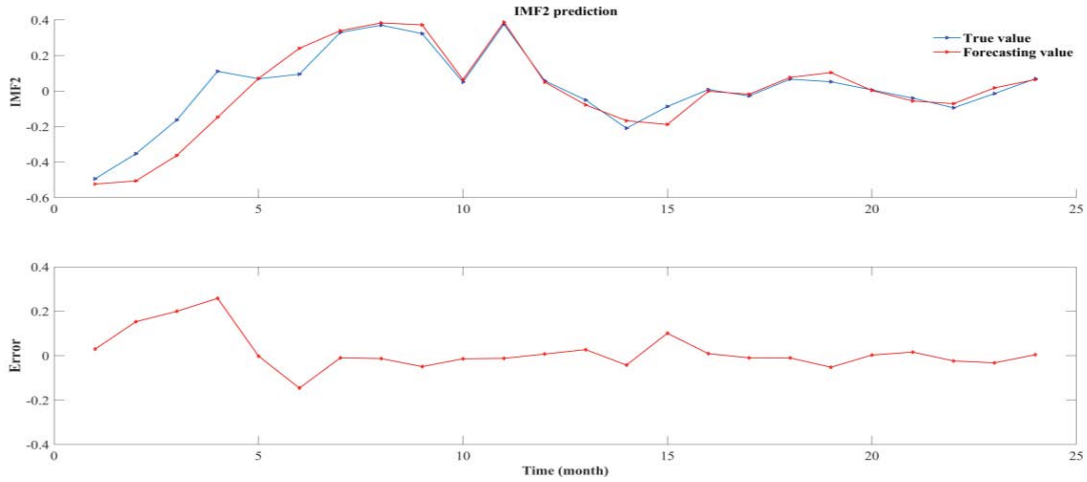

(b)

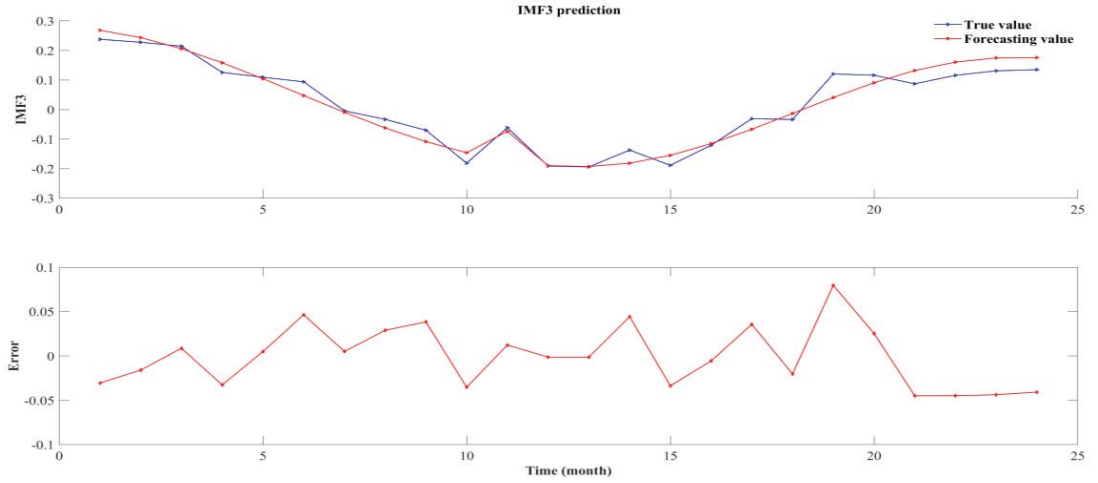

(c)

Fig. 5. The prediction results of IMF1 ~ IMF6 and residual. (a) IMF1 forecast results and errors, (b) IMF2 forecast results and errors, (c) IMF3 forecast results and errors.

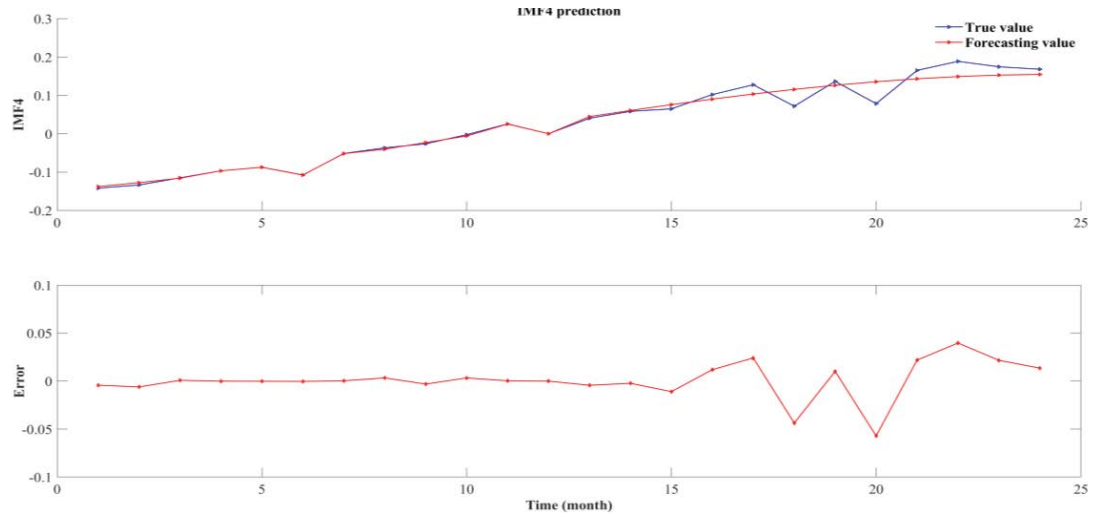

(d)

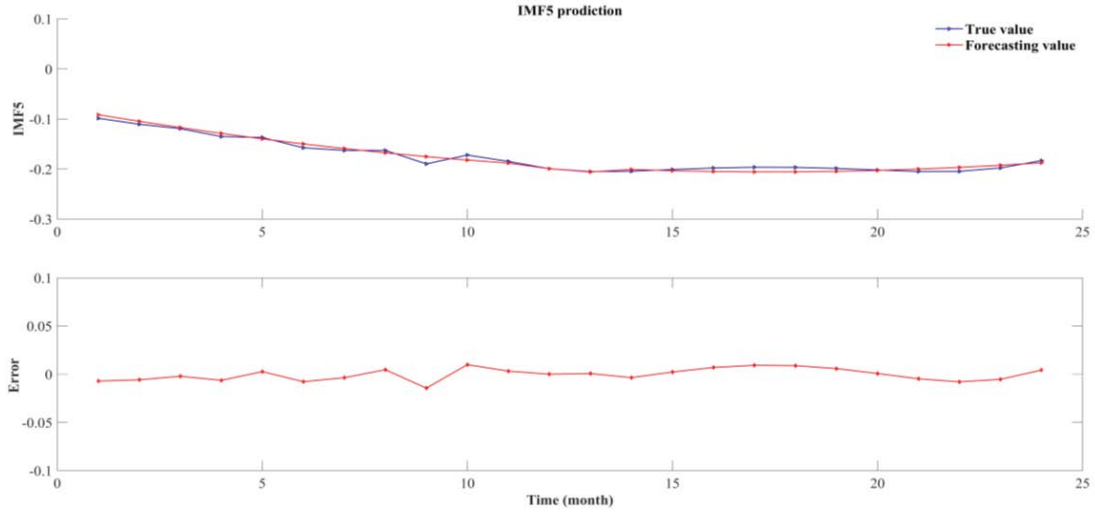

(e)

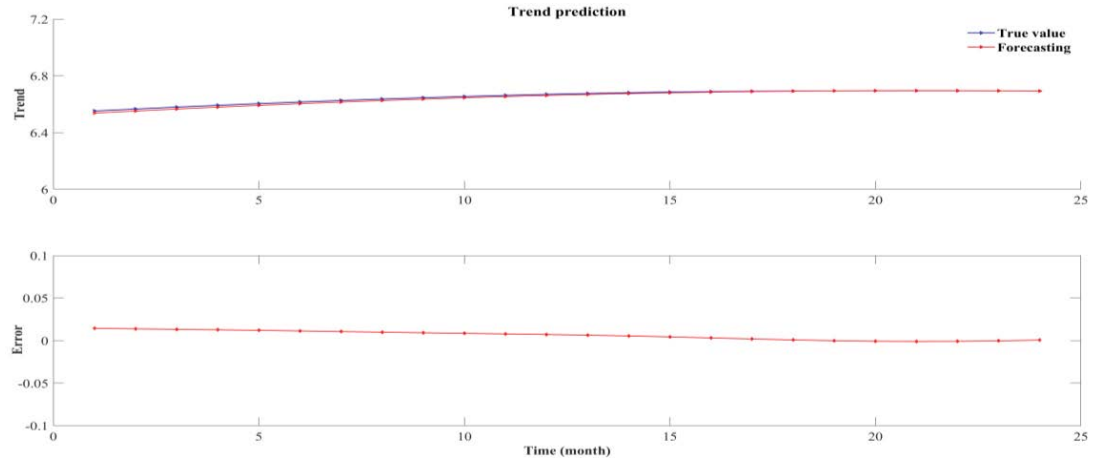

(f)

Fig. 5. The prediction results of IMF1 ~ IMF6 and residual. (d) IMF4 forecast results and errors, (e) IMF5 forecast results and errors, and (f) trend prediction results and errors.

Table 1
Relative error index of IMF1 ~ residual

Forecast	Maximum relative error (%)	Relative error minimum (%)	Relative error average (%)
IMF1	594.74	4.30	161.55
IMF2	287.17	1.50	41.30
IMF3	9.89	0.12	2.90
IMF4	1.88	0.05	0.67
IMF5	3.37	0.43	0.77
Trend item	0.04	0.00	0.01

Table 2
Relative error of groundwater depth prediction in People's Victory Canal Irrigation District from 2012 ~ 2013

Year	Month	True value (m)	Predicted value (m)	Absolute error (%)	Relative error (%)
2012	1	6.03	6.07	0.044	0.73
	2	6.21	6.23	0.022	0.35
	3	6.4	6.40	0.003	0.05
	4	6.49	6.54	0.045	0.69
	5	6.6	6.66	0.061	0.91
	6	6.83	6.76	–0.071	1.04
	7	6.6	6.65	0.051	0.77
	8	6.52	6.50	–0.023	0.35
	9	6.48	6.50	0.023	0.35
	10	6.56	6.59	0.031	0.47
	11	6.57	6.54	–0.029	0.44
	12	6.59	6.40	–0.194	3.04
2013	1	5.96	6.02	0.058	0.96
	2	5.86	5.91	0.052	0.88
	3	6.06	6.06	–0.002	0.03
	4	6.3	6.48	0.175	2.71
	5	6.71	6.77	0.055	0.81
	6	6.96	6.91	–0.046	0.67
	7	6.78	6.77	–0.008	0.13
	8	6.62	6.62	0.003	0.04
	9	6.8	6.78	–0.024	0.35
	10	6.8	6.81	0.012	0.17
	11	6.92	6.86	–0.055	0.80
	12	6.87	6.82	–0.052	0.77
Average relative error (%)		0.73			
Nash efficiency coefficient		0.96			

non-stationarity of the original sequence and have more regularity, which provides good conditions for BP model prediction.

2. Based on the CEEMD decomposition of the groundwater depth sequence, the BP network is used to predict the IMF1 ~ trend item, which solves the problem that the BP network cannot be used to learn some high-frequency mutation data directly. By predicting and reconstructing each component after CEEMD decomposition, the true value can be better fitted. Compared with the traditional single BP network, the model can reasonably reflect the real changes of the sequence in detail. The CEEMD-BP coupling model predicts a relative error of 0.73%, and calculates the Nash efficiency coefficient commonly used to verify the simulation results of the hydrological model. The result is 0.96, which has a higher accuracy and is better than the EEMD-BP model and BP neural network. This shows that the CEEMD-BP coupling model is feasible and reliable for the prediction of groundwater depth in irrigation areas.
3. The CEEMD-BP coupled model has an effective decomposition algorithm and a powerful, fast and stable prediction tool. The decomposition of groundwater burial depth series using the CEEMD method helps to understand the

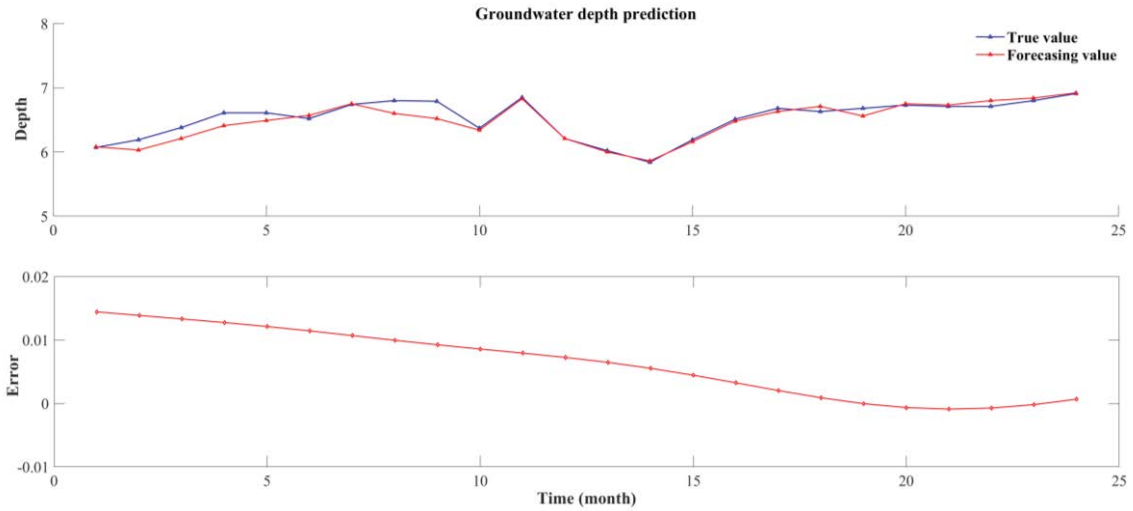

Fig. 6. The groundwater depth prediction curve of People's Victory Canal Irrigation District from 2012 ~ 2013.

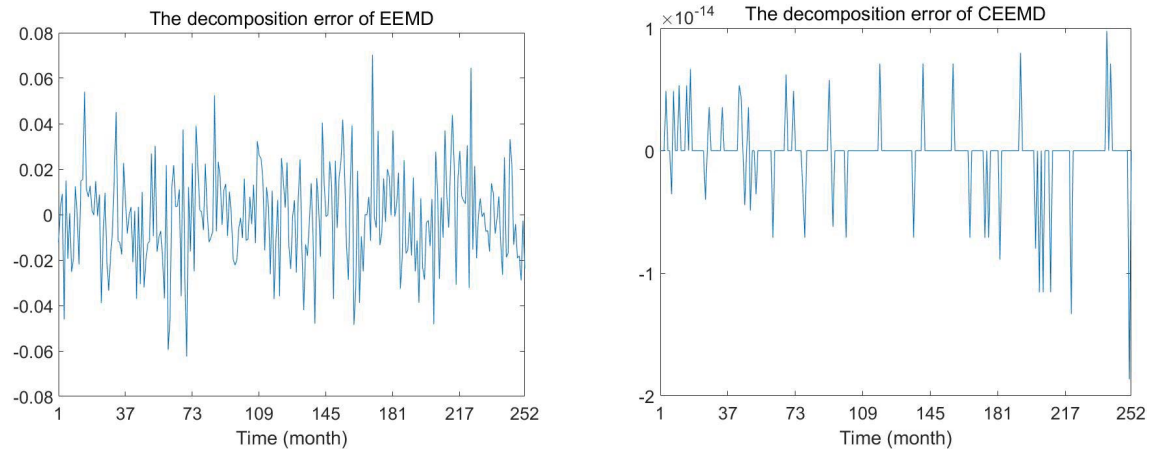

Fig. 7. CEEMD, EEMD reconstruction error.

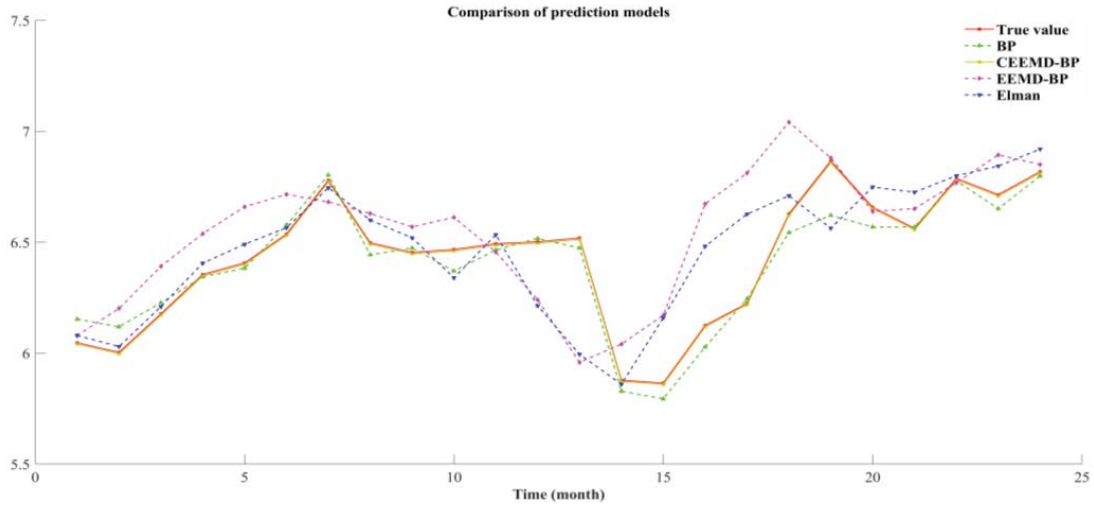

Fig. 8. The CEEMD-BP model is compared with other models.

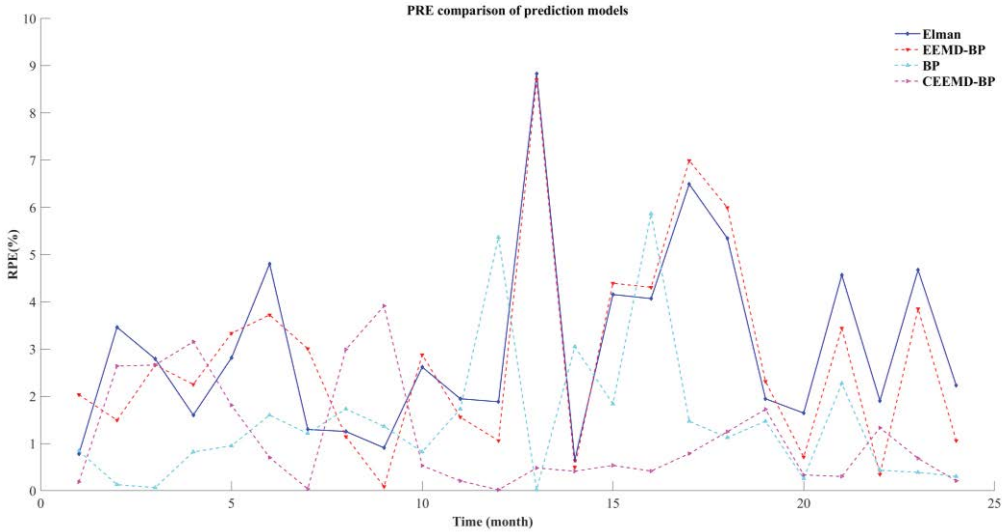

Fig. 9. The CEEMD-BP model is compared with other models.

Table 3
CEEMD-BP model is compared with other models

Predictive model	MAE (m)	RMSE (m)	MAPE (%)
CEEMD-BP	0.047	0.242	0.730
EEMD-BP	0.095	0.485	1.469
BP	0.184	0.929	2.819
Elman	0.198	0.997	3.027

characteristics of groundwater burial period changes, and can transform non-linear and non-smooth time series into smooth time series, which helps to improve the accuracy of prediction, solving the problem that it is difficult to reveal the characteristics of groundwater burial depth changes and the low prediction accuracy by using BP model prediction alone, and has broad application prospects. The prediction algorithm based on the CEEMD-BP model can be used not only for groundwater burial depth prediction, but also for the prediction of other time series such as rainfall, runoff and meteorological factors.

4. Although the overall prediction accuracy of the established CEEMD-BP coupled model is high, there are also shortcomings, such as the network parameters need to be set and adjusted artificially, the study only made short-term prediction of groundwater depth of burial, but not long-term prediction, in addition, the model does not involve the influence of physical mechanism of groundwater depth of burial change, its applicability and accuracy improvement still need further research, these will be the next research direction These will be the next research directions and priorities.

Acknowledgements

This work is financially supported by Technology Research Center of Water Environment Governance and Ecological Restoration Academician Workstation of Henan Province, Program for Science & Technology Innovation Talents in Universities of Henan Province (No. 15HASTIT049).

Data availability statement

All relevant data are included in the paper or it's Supplementary Information.

References

[1] J.T. Huang, Research on the Response Mechanism of Evapotranspiration in Semi-arid Area to Groundwater Changes, J. Chang'an University, 2013.
[2] C.W. Chai, Z.R. Jiang, X.Y. Xu, W.D. Tang, W.W. Chai, L.J. Li, C.X. Li, Determination of land desertification types in the desert oasis transition zone in Minqin County, J. N. Forest. Univ., 6 (2006) 12–16.
[3] Y. Qiao, X.J. Liang, Y.B. Wang, Application and comparative study of two models in groundwater burial depth prediction, Water Con. Irrig., 3 (2014) 45–47, 53.
[4] C.H. Xiao, Y.G. Hao, P.Y. Jia, Changes of water factors in Dengkou Oasis in the northeast of Ulan Buhe Desert in recent 52 years, Ari. Land Res. Environ., 6 (2008) 161–165.
[5] P.P. Adhikary, Ch.J. Dash, Comparison of deterministic and stochastic methods to predict spatial variation of groundwater depth, Appl. Sci., 7 (2017) 339–348.
[6] K. Al-Mahallawi, J. Mania, A. Hani, I. Shahrour, Using of neural networks for the prediction of nitrate groundwater contamination in rural and agricultural areas, Environ. Earth Sci., 65 (2012) 917–928.
[7] P. Sucharita, K. Shiv, Y. Kumar, C.S. Harish, Assessment of groundwater utilization status and prediction of water table depth using different heuristic models in an Indian interbasin, J. Soft Comput., 23 (2019) 10261–10285.
[8] M. Khorasani, M. Ehteshami, H. Ghadimi, M. Salari, Simulation and analysis of temporal changes of groundwater depth using time series modeling, Model. Earth Syst. Environ., 2 (2016) 90, doi: 10.1007/s40808-016-0164-0.
[9] P.R. Maiti, J. Medha, M.S. Sabita, Comparative analysis of performance of neural network and neuro-fuzzy model in prediction of groundwater table fluctuation, Int. J. Hydrol. Sci. Technol., 2 (2012) 252–269.

[10] D. Liu, G.X. Li, Q. Fu, M. Li, C.L. Liu, A.F. Muhammad, I.K. Muhammad, T.X. Li, S. Cui, Application of particle swarm optimization and extreme learning machine forecasting models for regional groundwater depth using nonlinear prediction models as preprocessor, J. Hydrol. Eng., 23 (2018), doi: 10.1061/(ASCE)HE.1943-5584.0001711.
[11] T. Zhou, F.X. Wang, Z. Yang, Comparative analysis of ANN and SVM models combined with wavelet preprocess for groundwater depth prediction, Water, 9 (2017) 781, doi: 10.3390/w9100781.
[12] G.-C. Shao, K. Zhang, Z.-Y. Wang, X.-J. Lu, Groundwater depth prediction model based on IABC-RBF neural network, J. Zhejiang Univ. (Eng. Sci.), 53 (2019) 1323–1330.
[13] C.F. Zhang, H.R. Chen, Z.Q. Yue, Groundwater burial depth simulation prediction based on long and short term memory network (LSTM) - an example analysis of Guanzhong Plain, Chin. Rur. Water Con. Hydro., (2020) 127–131+137.
[14] H.J. Yu, X.H. Wen, Q. Feng, Z.L. Yin, Z.Q. Chang, T.F. Yu, X.Y. Niu, Using wavelet transform and support vector machine coupling model (WA-SVM) to predict groundwater depth in arid areas, Chin. Des., 36 (2016) 1435–1442.
[15] Q.Z. Liang, L.Q.L.D. Wang, G.G. Li. Regional groundwater burial depth PSO-ELM prediction model based on EEMD, Water Res. Hydrol. Technol., 51 (2020) 45–51.
[16] J.R. Zhang, H.M. Tang, T. Wen, J.W. Ma, Q.W. Tan, D. Xia, X. Liu, Y.Q. Zhang, A hybrid landslide displacement prediction method based on CEEMD and DTW-ACO-SVR—cases studied in the Three Gorges Reservoir Area, Sensors, 20 (2020) 4287, doi: 10.3390/s20154287.
[17] Y.T. Sang, X.H. Zhao, X.P. Zhu, D.J. Xi, Monthly runoff prediction of the upper Fen River based on CEEMD- BP model, Yellow River, 41 (2019) 1–5.
[18] N.E. Huang, Z. Shen, S.R. Long, M.C. Wu, H.H. Shih, Q.N. Zheng, N.-C. Yen, C.C. Tung, H.H. Liu, The empirical mode decomposition and the Hilbert spectrum for nonlinear and non-stationary time series analysis, Proc. R. Soc. London, Ser. A, 454 (1998) 903–995.
[19] J.-R. Yeh, J.-S. Shieh, N.-E. Huang, Complementary ensemble empirical mode decomposition: a novel noise enhanced data analysis method, Adv. Adapt. Data Anal., 2 (2010) 135–156.
[20] J. Wang, W.D. Li, Ultra-short-term wind speed prediction based on CEEMD and GWO, Pow. Sys. Pro. Con., 46 (2018) 69–74.
[21] X. Chen, X.F. Wang, W.Y. Qi, T. Zhou, Application of BP neural network model based on genetic algorithm in groundwater depth prediction: taking Mengcheng County as an example, Water Res. Hydrol. Technol., 49 (2018) 1–7.
[22] B. Zhang, J.M. Liu, Groundwater dynamic prediction based on BP neural network, Res. Soil. Water Con., 19 (2012) 235–237.
[23] L. Xu, P. Li, Aero-engine performance parameter prediction based on dynamic neural network, J. Binzhou Univ., 31 (2015) 23–27.